ELSEVIER

Journal of Crystal Growth 164 (1996) 248–255

JOURNAL OF CRYSTAL GROWTH

Initial growth stages of $Al_xGa_{1-x}P$ on epitaxial silicon

C.J. Santana *, C.R. Abernathy, S.J. Pearton, K.S. Jones

Department of Materials Science and Engineering, University of Florida, Gainesville, Florida 32611, USA

Abstract

The nucleation and growth of $Al_xGa_{1-x}P$ grown by metalorganic molecular beam epitaxy on epitaxial Si(100) substrates was studied by high-resolution transmission electron microscopy and atomic force microscopy. It was found that for deposition temperatures in the range 450–550°C, the $Al_xGa_{1-x}P$ grew by three-dimensional island growth for all compositions studied ($x = 0$ to 0.45). Changes in aluminum concentration have been found to affect the density and size distributions of the $Al_xGa_{1-x}P$ islands. In addition, increases in both temperature and composition have been shown to lead to bimodal distributions of islands.

1. Introduction

Compound semiconductors grown on Si substrates are attractive for increasing wafer diameter and strength as well as for monolithic integration of optoelectronic and microelectronic devices. In order to realize these applications the heteroepitaxial growth of the compound semiconductor must result in an epilayer with few defects for optimum device efficiency, and a smooth surface morphology for the growth of planar device structures. However, growth of compound semiconductors on silicon is very difficult due to several factors including lattice mismatch, thermal coefficient mismatch, polar on non-polar growth, substrate preparation and chemical differences (i.e. differences in interfacial and surface energies). These factors can influence the defect density and the growth mode of the epilayers. In fact, layer-by-layer growth is obtained for only a limited number of film/substrate materials combinations under select growth conditions [1]. The more common observation is that the deposited material forms three-dimensional islands [2]. Islands may form directly on the bare substrate, in the Volmer–Weber growth mode [3], or on top of a very thin but uniform film in the Stranski–Krastanov growth mode [3]. Island growth is undesirable for the fabrication of planar device structures because surface morphologies of the resulting films tend to be very rough. Additionally, defects are introduced into the epilayers during island growth and coalescence [4]. As one might expect, the strength of the film/substrate interaction and the lattice mismatch of the film and substrate have an influence on the growth mode. Therefore, materials with strong bonds to the substrate and a small lattice mismatch are often sought to minimize or eliminate island growth. In the $Al_xGa_{1-x}P$/Si material system, the lattice mismatch

* Corresponding author. Fax: +1 352 846 0403; E-mail: sandman@grove.ufl.edu.

SSDI 0022-0248(95)01058-0

varies from 0.36–0.37% for $x = 0$ to 1 ($a_{GaP} = 5.4505$ Å, $a_{AlP} = 5.451$ Å, and $a_{Si} = 5.4307$ Å). The strong interaction between aluminum and silicon may reduce epilayer surface roughness as found in other heteroepitaxial systems [5,6]. To reduce the effects of island formation, a kinetically limited two-step growth technique can also be employed in which low deposition temperatures are used to establish a thin planar nucleation layer prior to the growth of the final active layer at a higher growth temperature. George et al. [7] used the $Al_xGa_{1-x}P$ system to reduce the effects of island nucleation in the growth of MOCVD GaAs/AlGaP/Si(100) by using the ternary as a planarizing buffer layer without the use of a low growth temperature. Additions of Al to GaP were found to induce planar growth as a result of the stronger bonding between Al–Si as compared to the Ga–Si bond. No evidence of island formation could be found for Al concentrations of $x > 0.4$.

To date, the nucleation and growth mode of the $Al_xGa_{1-x}P$ material system has not been clarified and this knowledge may help further the progress towards integration of optical and electronic devices. In addition, a better understanding of the influence of materials parameters and growth conditions on the morphology of $Al_xGa_{1-x}P$ on silicon may help identify the conditions for optimum buffer layer formation. In this article, we investigate the initial growth processes of $Al_xGa_{1-x}P$ layers on Si(100) substrates grown by MOMBE.

2. Experimental procedure

$Al_xGa_{1-x}P$ was deposited on 2″ epitaxial silicon wafers using a Varian gas source GEN II system. The wafers were obtained commercially through Silicon Quest International and were p-type with 1 μm of epitaxial silicon. Substrate preparation consisted of etching the wafers in a HF:DI solution (1:50 by volume) for 15 s, followed by a DI rinse for 15 s, and a nitrogen dry off. The wafers were exposed to room air for no more than 15 min before entry into the load-lock chamber where a pressure of $\sim 10^{-6}$ Torr was achieved. Dimethylethylamine alane (DMEAA), triethylgallium (TEG), and precracked PH_3 (1000°C) were used as the group III and V precursors. $Al_xGa_{1-x}P$ was deposited on the In-free mounted silicon wafers at growth pressures of $\sim 2 \times 10^{-5}$ Torr and at growth temperatures of 450, 500 and 550°C as monitored by a calibrated optical pyrometer. The ternary composition was varied by changing the group III precursor flow rates to grow compositions of $x = 0$, 0.15, 0.3, and 0.45. Growth rates (2.5–4.0 Å/s) and precursor flow rates for each composition and temperature were determined previously from growth of 1 μm thick films. Flows of the group III precursors were maintained such that the growth rates for each composition were constant at each growth temperature while the group V flow rate was maintained at 2 sccm. Growth times ranged from ~13 to 19 s for the deposition of approximately 50 Å mean coverage of material on the silicon wafers. Characterization of the nucleated $Al_xGa_{1-x}P$ was performed on a JEOL 4000FX HRTEM using cross-sectional imaging at 400 kV, and on a Digital Instruments Multimode Nanoscope III AFM (tapping mode). The cross-sectional TEM samples were prepared by cutting the wafers parallel to [110] planes, followed by lapping with 5 μm alumina powders and ion milling to electron transparency. Analysis of raw AFM nucleation data was accomplished by using the grain size analysis software module of the Nanoscope III package. Nucleation data were obtained by defining a height threshold for a plane that sections the three-dimensional data at the defined height resulting in a plane of sectioned features (islands). The number and mean area of the sectioned islands within the plane are calculated by the computer for each height threshold.

3. Results and discussion

3.1. High resolution transmission electron microscopy

Cross-sectional transmission electron microscopy (XTEM) was used to image the nucleated $Al_xGa_{1-x}P$ on silicon. Discrete island formation was observed for all compositions at each growth temperature studied. At 450°C, the islands appeared to be quite dense and fairly uniform in height (50–90 Å) as shown in Figs. 1a and 1b. Island densities could not be obtained accurately from the XTEM micrographs however, due to both island overlap and an unknown

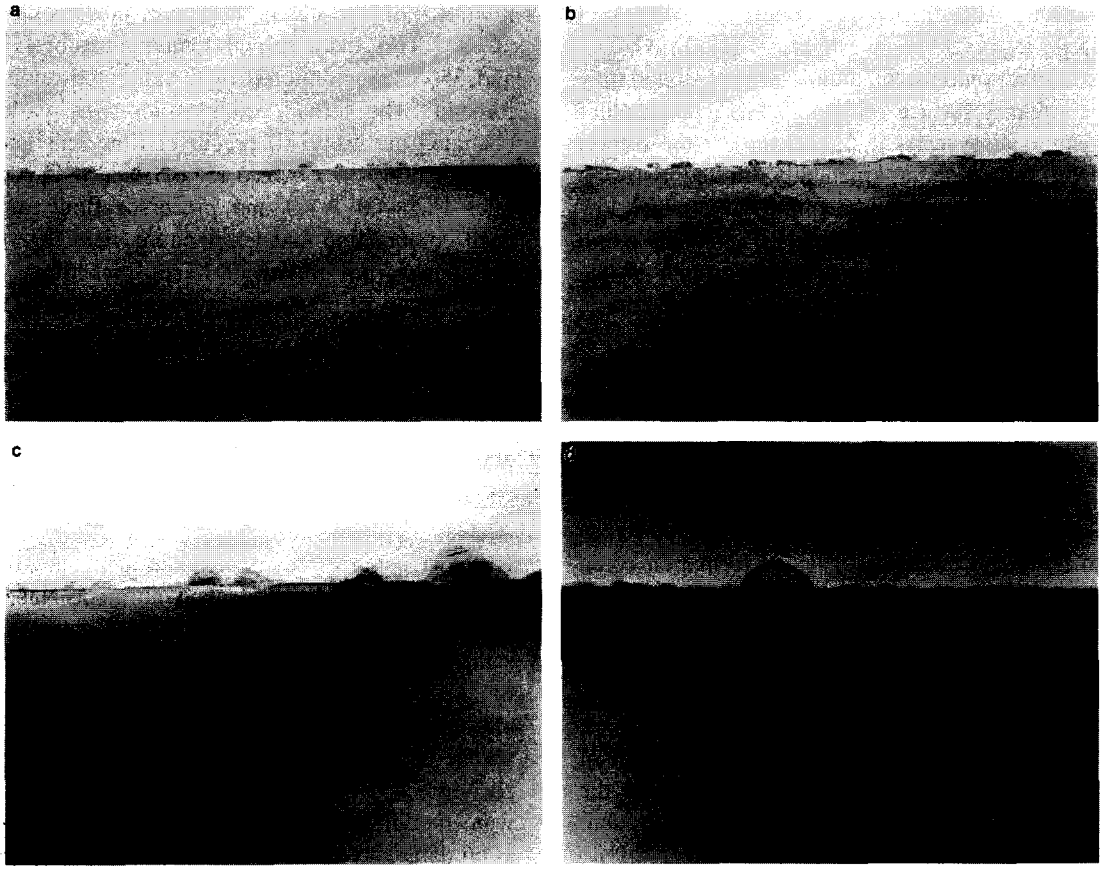

Fig. 1. Cross-sectional HRTEM images of $Al_xGa_{1-x}P/Si$ (200KX); (a) GaP/Si, $T_G = 450°C$, (b) $Al_{0.15}Ga_{0.85}P/Si$, $T_G = 450°C$, (c) GaP/Si, $T_G = 550°C$, and (d) $Al_{0.45}Ga_{0.55}P/Si$, $T_G = 550°C$.

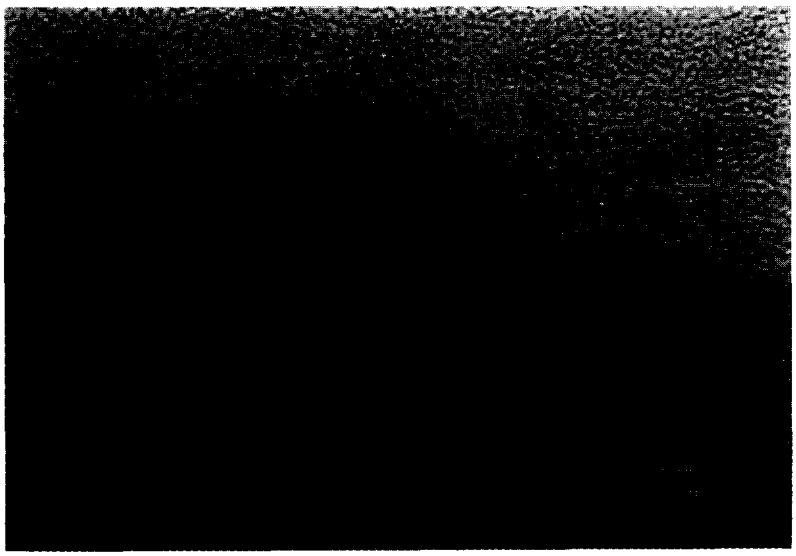

Fig. 2. Cross-sectional HRTEM image of an $Al_xGa_{1-x}P$ island (4MX). Planar defects exist in many of the islands and appear to nucleate at areas of disorder at the heterointerface.

specimen thickness. Instead, AFM imaging was used to obtain island density data. As the growth temperature was increased, the GaP islands were found to increase in both size and distribution (Fig. 1c). $\{111\}$ faceting of the GaP islands [8] occurred at each growth temperature and was especially pronounced at 550°C. Defects in the islands, even at these early stages of growth, were identified to be stacking faults and microtwins. For compositions of $x > 0$ and growth temperatures (T_G) greater than 450°C, islands having dimensions quite different from the low growth temperature islands were observed (Fig. 1d), while the existence of the fairly uniform smaller islands was maintained. At 500°C, larger islands were found for each composition except for $x = 0.15$, and at 550°C, the larger islands were present for all Al containing compositions. Imaging of the larger islands in HRTEM was difficult because of their scarcity. It was later discovered by AFM imaging that the large island population was an order of magnitude less than that of the smaller islands. The large islands were also found to be separated from the smaller islands by areas of apparent bare silicon substrate.

There was good registry across the island/substrate interface in all cases. Island faceting and two-dimensional defects were found to occur in islands of all sizes as shown in Fig. 2. Planar defects are commonly attributed to lattice mismatch and thermal expansion mismatch stresses between the film and

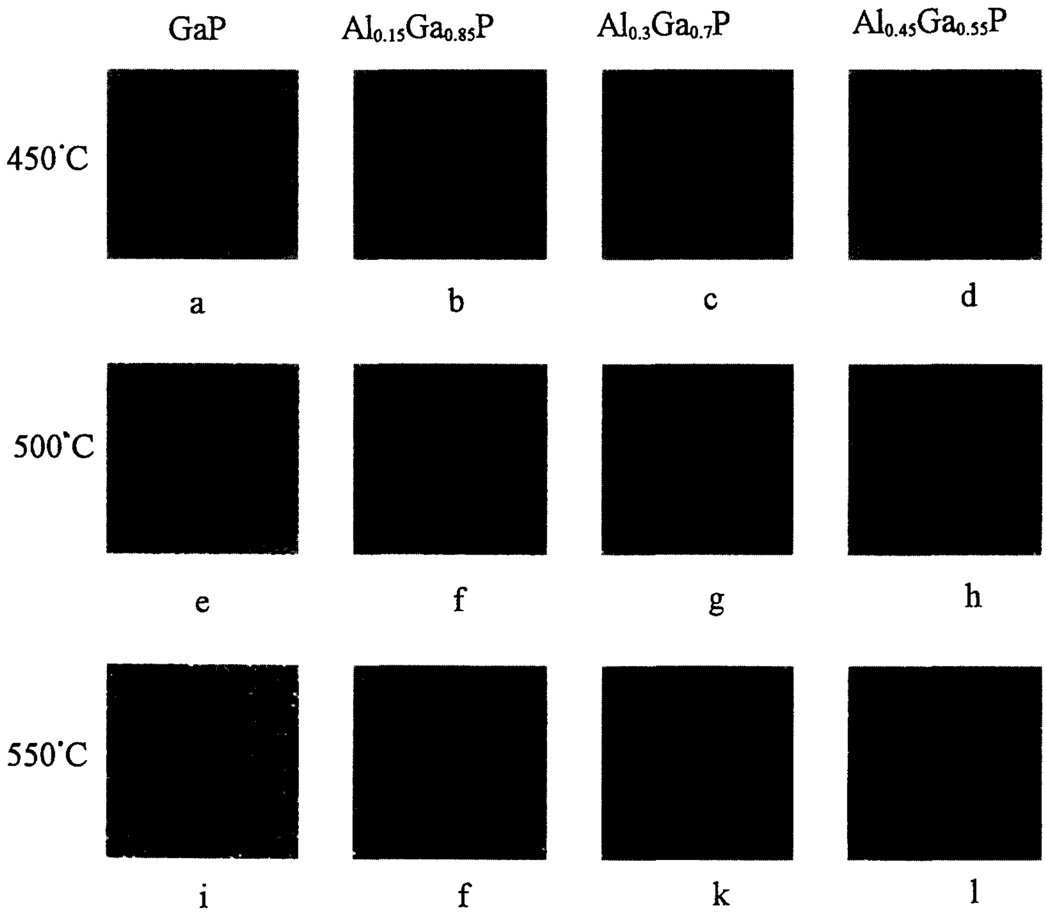

Fig. 3. Normal incidence AFM images of $Al_xGa_{1-x}P/Si$ (25 μm^2 scans).

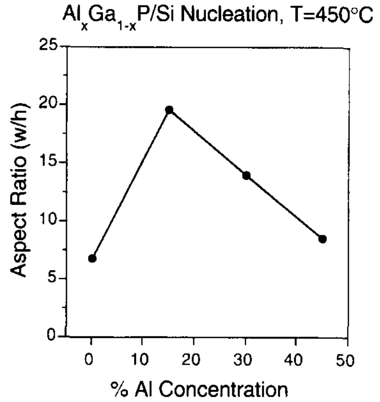

Fig. 4. Aspect ratio (width/height) of $Al_xGa_{1-x}P$ islands deposited on silicon at 450°C.

substrate. Stacking fault formation has been reported to occur by the nucleation and subsequent separation of Shockley partial from dissociated dislocations as a result of mismatch stresses [9]. However, Ernst and Pirouz [8] have reported that the mismatch stresses play only a minor role in the formation of the planar defects and that the dominate formation mechanism is atomic deposition errors on {111} island facets in the early stages of growth. It should be noted that planar defects that occurred in the $Al_xGa_{1-x}P$ islands with heights of 50–500 Å, existed well below the critical thickness of ≥ 1500 Å for this material system. The critical thickness for $Al_xGa_{1-x}P$/Si was calculated using the People and Bean [10] equations assuming a Shockley partial dislocation with a Burgers vector of $\boldsymbol{b} = a/6\langle 112 \rangle$. The planar defect formation mechanism for this material system was not studied in our investigation, but it was observed that many two-dimensional defects appeared to originate from areas of disorder at the interface as shown in Fig. 2. Areas of disorder at the interface as observed by HRTEM can be attributed to strain

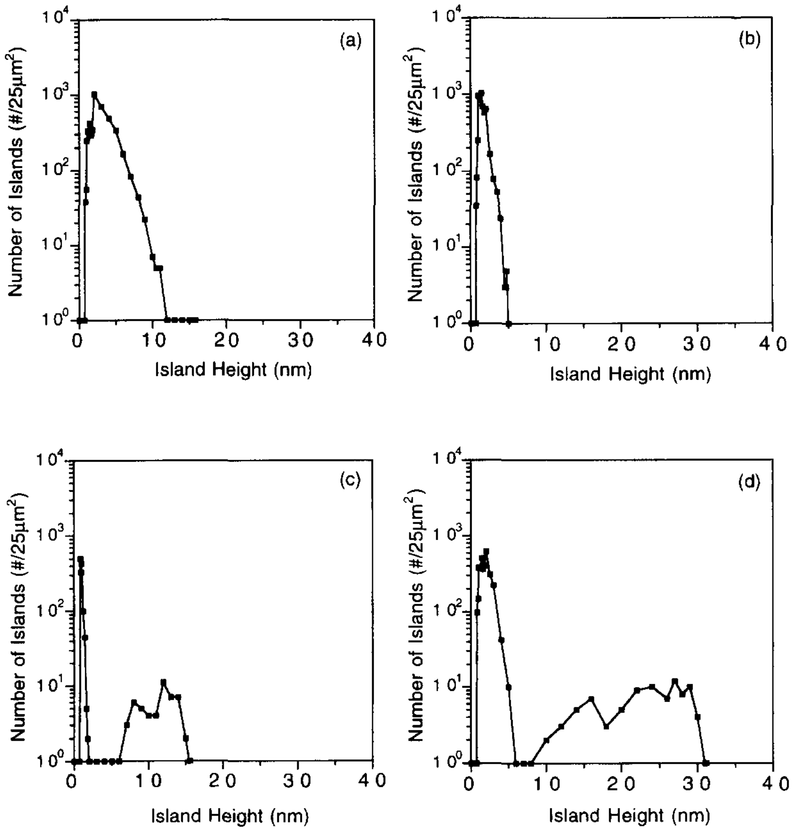

Fig. 5. Island size histograms for nucleation of $Al_xGa_{1-x}P$ from 25 μm² scans (a) GaP/Si, $T_G = 450°C$, (b) $Al_{0.15}Ga_{0.85}P$/Si, $T_G = 450°C$, (c) $Al_{0.45}Ga_{0.55}P$/Si, $T_G = 500°C$, and (d) $Al_{0.45}Ga_{0.55}P$/Si, $T_G = 550°C$.

caused by interfacial defects [11] or by residual contamination such as an oxide or a carbide [12,13].

3.2. Atomic force microscopy

In Fig. 3 we show normal incidence, atomic force microscope (AFM) images of the $Al_xGa_{1-x}P$ specimens. The AFM images were used in collaboration with the HRTEM to better understand and view the nucleation processes as well as to obtain island size and distribution data. Both HRTEM and AFM imaging revealed the growth mode of MOMBE deposited $Al_xGa_{1-x}P$ on silicon to be island type for all compositions. These results contrasted with the findings of George et al. [7]. They had found that additions of Al to the $Al_xGa_{1-x}P$/Si system grown by MOCVD had suppressed the tendency for island formation. In the MOMBE grown $Al_xGa_{1-x}P$, aluminum was found to play a role in the modification of the island size and density distributions, but did not induce planar growth. It is speculated that the existence of a boundary layer in MOCVD may enhance planar growth conditions.

At 450°C, the $Al_xGa_{1-x}P$ islands were small and fairly uniform with average heights in the range 50–90 Å (as measured from HRTEM micrographs) and aspect ratios (island width/height) that peaked at 15%Al in $Al_xGa_{1-x}P$ grown at 450°C as shown in Fig. 4. No evidence of larger islands was observed by HRTEM or AFM at this growth temperature. The island size histograms for nucleation at 450°C are plotted in Figs. 5a and 5b for GaP and $Al_{0.15}Ga_{0.85}P$, respectively. The size distribution of the islands was found to narrow upon addition of Al to GaP for $x \leq 0.3$, and then slightly broaden again for $x = 0.45$. The narrowing island distribution supports the argument for island suppression by the addition of aluminum due to the stronger bond of Al–Si than that of Ga–Si. However, the broadening of the island distributions with increased Al is contrary to this explanation and the mechanism for this behavior will be discussed later. At 500°C, a similar narrowing effect was observed as well as the onset of large islands for compositions $x \geq 0.3$ (see Fig. 5c). At 550°C, large islands were present for each composition (Fig. 5d). The large islands were not influenced greatly by the changes in composition at 550°C as found at 500°C.

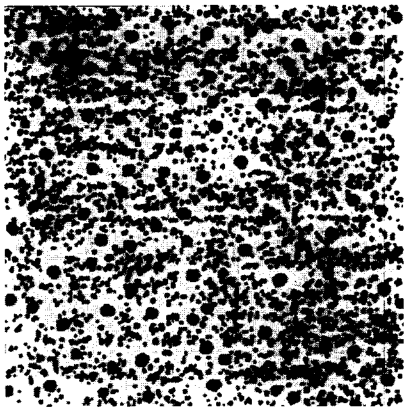

Fig. 6. AFM image of $Al_{0.15}Ga_{0.85}P$ grown at $T_G = 550$°C with large islands surrounded by depletion area (25 μm^2 scan).

Small island sizes remained fairly constant in the Al containing deposits as the formation of large islands occurred, creating a bimodal distribution of island sizes. The GaP island sizes however, had large size deviations which lead to broad island distributions. GaP did not show the presence of a bimodal size distribution, but the mean island sizes of the larger GaP islands were similar to the mean island sizes of the larger $Al_xGa_{1-x}P$ islands. Therefore, the formation of the bimodal distribution is believed to be a consequence of adding Al to GaP and may be an inherent part of the MOMBE deposition of $Al_xGa_{1-x}P$ using TEG and DMEAA.

As noted in the HRTEM data, AFM confirmed the existence of depletion zones around the larger islands. Fig. 6 shows an AFM image of $Al_{0.15}Ga_{0.85}P$ nucleated at 550°C with areas around the larger islands that are free of small islands. The formation of the larger islands may be occurring by an Ostwald ripening process [14] where the large islands grow at the expense of the smaller surrounding islands. This process cannot be verified at this time however because we have only examined growth of each composition at one interval of time. To observe the Ostwald process one needs to examine growth over several periods of time to first confirm the existence of small islands and then to witness the disappearance of these smaller islands in the vicinity of larger growing islands.

Given the presence of large islands, the question then is what is the driving force for their formation.

Growth modes of heteroepitaxial systems depend on lattice mismatch and interface free energy terms [15]. Since Al–Si bonding is stronger than Ga–Si bonding one would expect to see growth occurring as we saw for $Al_xGa_{1-x}P$ at 450°C or as George et al. [7] had reported for MOCVD grown $Al_xGa_{1-x}P$ on silicon. However, island suppression was not observed as the Al concentration was increased in the MOMBE deposited $Al_xGa_{1-x}P$ for growth temperatures ≥ 500°C. The lattice mismatch of the $Al_xGa_{1-x}P/Si$ system is relatively unchanged as x is increased from 0 to 0.45 (mismatch changes less than a tenth of a percent). Therefore, a significant driving force arising from lattice mismatch is not expected.

The formation of the larger islands and the depletion regions surrounding them suggest that the surface mobility of the adatoms or adsorbed molecules may be enhanced. This mobility enhancement may arise from the gettering of adsorbed ethyl radicals by the Al adatoms. Ethyl radicals are believed to be adsorbed to the substrate surface as part of the decomposition process of TEG as reported by Robertson et al. [16]. In addition, carbon incorporation in GaAs has been shown to increase with the presence of aluminum [17,18]. It is proposed that the Al adatoms getter adsorbed ethyl radicals from the TEG decomposition process, weakening the Al–Si substrate bond, and allowing the Al to move more freely on the surface. Lee et al. [18] used quadrupole mass spectroscopy to analyze the desorption mass spectra from the growth of AlGaAs in MOMBE using TEG and elemental Al. They found a large increase in the $m/e = 57$ and 85 peaks when the populated GaAs surface was exposed to an elemental Al flux. These peaks were attributed to $H \cdot Al \cdot C_2H_5$ and $Al(C_2H_5)_2$ and were explained by the transfer of ethyl groups from the gallium species to atomic aluminum. The Al gettering effect may also increase the mobility of the Ga species by decreasing site blocking by ethyl radicals. Thick $Al_xGa_{1-x}P$ films grown by MOMBE were analyzed by secondary ion mass spectroscopy and found to increase in carbon concentration with increase aluminum content for each growth temperature. To help understand the mechanism for enhanced surface mobility of group III adatoms in the $Al_xGa_{1-x}P/Si$ system, alternative group III sources will be explored.

4. Conclusions

We have investigated for the first time the compositional and temperature dependence of the early stages of growth of $Al_xGa_{1-x}P$ on Si by MOMBE. For $x = 0$ to 0.45 and at a nominal 50 Å deposition, $Al_xGa_{1-x}P$ grows by the Volmer–Weber growth mode on the Si surface in the temperature range 450–550°C. Additions of Al to GaP at temperatures ≥ 500°C has been shown to influence the nucleation behavior by the formation of a bimodal distribution of island sizes. Increased concentrations of Al in $Al_xGa_{1-x}P$ were not found to induce planar growth even for $x > 0.4$ at any growth temperature studied and in fact lead to a more severe islanding effect.

Acknowledgements

This work is performed in both the MAIC and Microfabritech facilities. We would like to thank the staff at Microfabritech, especially Maggie Puga-Lambers, and their director, Dr. P.H. Holloway, for their support.

References

[1] Falta, M.C. Reuter and R.M. Tromp, Appl. Phys. Lett. 65 (1994) 1680.
[2] J.E. Northrup, Phys. Rev. Lett. 62 (1989) 2487.
[3] E. Bauer, Z. Krist. 110 (1958) 423.
[4] S. Guha, H. Munekata, F.K. LeGoues and L.L. Chang, Appl. Phys. Lett. 60 (1992) 3220.
[5] V. Alberts, J. Crystal Growth 140 (1994) 299.
[6] C.R. Abernathy, J.D. MacKenzie, S.R. Bharatan, K.S. Jones and S.J. Pearton, J. Vac. Sci. Technol. A 13 (1995) 716.
[7] T. George, E.R. Weber, S. Nozaki, A.T. Wu, N. Noto and M. Umeno, J. Appl. Phys. 67 (1990) 2441.
[8] F. Ernst and P. Pirouz, J. Mater. Res. 4 (1989) 834.
[9] P.M.J. Marée, J.C. Barbour, J.F. v.d. Veen, K.L. Kavanagh, C.W.T. Bulle-Lieuwma and M.P.A. Viegers, J. Appl. Phys. 62 (1987) 4413.
[10] R. People and J.C. Bean, Appl. Phys. Lett. 47 (1985) 322.
[11] M. Akiyama, Y. Kawarada, S. Nishi, T. Ueda and K. Kaminishi, Heteroepitaxy on Silicon (Materials Research Society, Palo Alto, 1986) p. 53.
[12] J.M. Olson, M.M. Al-Jassim, A. Kibbler and K.M. Jones, J. Crystal Growth 77 (1986) 515.

[13] A.E. Blakeslee, M.M. Al-Jassim and S.E. Asher, Heteroepitaxy on Silicon II (Materials Research Society, San Francisco, 1987) p. 105.

[14] M. Zinke-Allmang, L.C. Feldman and S. Nakahara, Appl. Phys. Lett. 51 (1987) 975.

[15] D.J. Eaglesham, H.-J. Gossmann and M. Cerullo, Epitaxial Heterostructures (Materials Research Society, San Francisco, 1990) p. 51.

[16] A. Robertson, Jr., T.H. Chiu, W.T. Tsang and J.E. Cunningham, J. Appl. Phys. 64 (1988) 877.

[17] C.R. Abernathy, D.A. Bohling and A.C. Jones, Advanced III–V Compound Semiconductor Growth, Processing and Devices (Materials Research Society, San Francisco, 1992) p. 3.

[18] B.J. Lee, Y.M. Houng, J.N. Miller and J.E. Turner, J. Crystal Growth 105 (1990) 168.